Title

T Cells Expressing CD19/CD20 Bispecific Chimeric Antigen Receptors Prevent Antigen Escape by Malignant B Cells

Journal

Cancer Immunology Research, 4(6)

ISSN

2326-6066

Authors

Zah, Eugenia
Lin, Meng-Yin
Silva-Benedict, Anne
et al.

Publication Date

2016-06-01

DOI

10.1158/2326-6066.cir-15-0231

Peer reviewed

Title: T cells expressing CD19/CD20 bi-specific chimeric antigen receptors prevent antigen escape by malignant B cells

Eugenia Zah[1], Meng-Yin Lin[1], Anne Silva-Benedict[2,3], Michael C. Jensen[2,4,5], Yvonne Y. Chen[1,*]

[1]Department of Chemical and Biomolecular Engineering, University of California—Los Angeles, 420 Westwood Plaza, Boelter Hall 5531, Los Angeles, CA 90095

[2]Ben Towne Center for Childhood Cancer Research, Seattle Children's Research Institute, 1100 Olive Way, Suite 100, Seattle, WA 98122

[3]Department of Oncology and Hematology, St. Luke's Regional Cancer Center, 1001 East Superior Street, Suite L101, Duluth, MN 55802

[4]Division of Pediatric Hematology-Oncology, University of Washington School of Medicine, 1100 Olive Way, Suite 100, Seattle, WA 98122

[5]Program in Immunology, Clinical Research Division, Fred Hutchinson Cancer Research Center, 1100 Olive Way, Suite 100, Seattle, WA 98122

Running Title: Bi-specific T cells prevent B-cell antigen escape

Keywords: Antigen escape, T-cell therapy, CD19 CAR, CD20 CAR, synthetic biology

Financial Support: National Institutes of Health (5DP5OD012133, grant to YYC; 2R01CA136551-06A1, grant to MCJ).

Corresponding Author: Yvonne Y. Chen, Department of Chemical and Biomolecular Engineering, University of California–Los Angeles, 420 Westwood Plaza, Boelter Hall 5531,

Los Angeles, CA 90095. Phone: (310) 825-2816. Fax: (310) 206-4107. Email: yvonne.chen@ucla.edu.

Conflicts of Interest: The authors declare competing financial interests in the form of a patent whose value may be affected by this publication. Michael C Jensen, MD, is a scientific co-founder, equity owner, and scientific advisory board member of Juno Therapeutics, Inc.

Word Count: 5485

Figures: 7 in main text; 7 in supplementary materials

Tables: 0 in main text; 1 in supplementary materials

Abstract

The adoptive transfer of T cells expressing anti-CD19 chimeric antigen receptors (CARs) has shown remarkable curative potential against advanced B-cell malignancies, but multiple trials have also reported patient relapses due to the emergence of CD19-negative leukemic cells. Here, we report the design and optimization of single-chain, bi-specific CARs that trigger robust cytotoxicity against target cells expressing either CD19 or CD20, two clinically validated targets for B-cell malignancies. We determined the structural parameters required for efficient dual-antigen recognition, and we demonstrate that optimized bi-specific CARs can control both wildtype B-cell lymphoma and CD19– mutants with equal efficiency *in vivo*. To our knowledge, this is the first bi-specific CAR capable of preventing antigen escape by performing true OR-gate signal computation on a clinically relevant pair of tumor-associated antigens. The CD19-OR-CD20 CAR is fully compatible with existing T-cell manufacturing procedures and implementable by current clinical protocols. These results present an effective solution to the challenge of antigen escape in CD19 CAR T-cell therapy, and they highlight the utility of structure-based rational design in the development of receptors with higher-level complexity.

Introduction

Adoptive T-cell therapy has demonstrated clinical efficacy against advanced cancers (1,2). In particular, multiple clinical trials have shown that T cells programmed to express anti-CD19 chimeric antigen receptors (CARs) have remarkable curative potential against relapsed B-cell malignancies (3-9). However, these trials have also revealed critical vulnerabilities in current CAR technology, including susceptibility to antigen escape by tumor cells (7,10). For example, a recent trial of CD19 CAR–T-cell therapy saw 90% of patients achieve complete remission, but 11% of those patients eventually relapsed with CD19-negative tumors (10). Antigen escape has also been observed in the adoptive transfer of T cells expressing NY-ESO1–specific T-cell receptors (11) and in cancer vaccine therapy for melanoma (12,13).

The probability of antigen escape by spontaneous mutation and selective expansion of antigen-negative tumor cells decreases with each additional antigen that can be recognized by the CAR-T cells. Therefore, a potential prophylaxis against antigen escape is to generate T cells capable of recognizing multiple antigens. Here, we present the rational design and systematic optimization of single-chain, bi-specific CARs that efficiently trigger T-cell activation when either of two pan–B-cell markers, CD19 or CD20, is present on the target cell. These novel CARs can be efficiently integrated into primary human T cells and administered in the same manner as CAR-T cells currently under evaluation in the clinic.

A single-chain, bi-specific CAR targeting CD19 and the human epidermal growth factor receptor 2 (HER2/neu) was previously reported by Grada et al. (14). This bi-specific receptor, termed TanCAR, efficiently triggered T-cell activation in response to either CD19 or HER2. However, since CD19 and HER2 are not typically expressed on the same cell, the TanCAR remains a proof-of-concept design. Importantly, Grada et al. highlighted that the TanCAR is less

strongly activated both *in vitro* and *in vivo* when challenged with target cells that express HER2 alone, as compared to HER2/CD19 double-positive targets (14). This observation suggests that tumor cells can still escape TanCAR detection by eliminating CD19 expression.

To effectively prevent antigen escape, the bi-specific CAR must not only recognize two antigens, but also process both signals in a true Boolean OR-gate fashion—i.e., either antigen input should be sufficient to trigger robust T-cell output. We thus refer to this particular type of bi-specific receptors as "OR-gate CARs." Here, we report on the development of CD19-OR-CD20 CARs, which trigger robust T-cell–mediated cytokine production and cytotoxicity when either CD19 or CD20 is present on the target cell. We demonstrate that the size and rigidity of CAR molecules can be calibrated to match the specific antigens targeted, and the optimal OR-gate CAR structure can be deduced from known structural requirements for single-input CARs. Finally, we show that the CD19-OR-CD20 CARs can control both wildtype and CD19– mutant B-cell lymphomas with equal efficiency *in vivo*, thus providing an effective safeguard against antigen escape in adoptive T-cell therapy for B-cell malignancies.

Materials and Methods

Plasmid construction. Bi-specific CD19-CD20 CARs were constructed by isothermal assembly (15) of DNA fragments encoding the CD19 single-chain variable fragment (scFv) derived from the FMC63 monoclonal antibody (mAb) (16), the CD20 scFv derived from the Leu-16 mAb (17), an IgG4-based extracellular spacer, the CD28 transmembrane domain, and the cytoplasmic domains of 4-1BB and CD3 zeta. Sequences of extracellular spacers and linkers connecting scFv domains are listed in Supplementary Table S1. All CARs were fused to a truncated epidermal

growth factor receptor (EGFRt) via a T2A peptide to facilitate antibody staining and sorting of CAR-expressing cells (18).

Cell-line generation and maintenance

Parental Raji cells were obtained from ATCC in 2003 and parental K562 cells were a gift from Dr. Laurence Cooper in 2001. Both cell lines were authenticated by short tandem repeat profiling at the University of Arizona Genetics Core in 2015. The Epstein-Barr virus transformed lymphoblastoid cell line (TM-LCL) was made from peripheral blood mononuclear cells as previously described (19). CD19+, CD20+, and CD19+/CD20+ K562 cells were generated by lentivirally transducing parental K562 cells with CD19 and/or CD20 constructs. CD19– Raji cells were generated by CRISPR/Cas9-mediated gene editing. Two million Raji cells were transiently transfected with 2 μg of CD19-CRISPR-T2A-NM plasmid using the Amaxa Nucleofection Kit V (Lonza) and the Amaxa Nucleofector 2b Device (Lonza). Twenty-four hours post-nucleofection, cells were co-incubated with 1.5 mg/mL G418 sulfate (Enzo Life Sciences) for 120 hours and further expanded in the absence of antibiotics for 11 days. CD19– cells were first enriched by staining cells with anti-CD19-APC followed by anti-APC microbeads (Miltenyi), and then removing labeled cells via magnetic bead-based cell sorting. A pure CD19– population was subsequently obtained by fluorescence-activated cell sorting using the FACSAria (II) at the UCLA Flow Cytometry Core Facility. All TM-LCL, Raji, and K562 cell lines were maintained in complete T-cell medium (RPMI-1640 (Lonza) with 10% heat-inactivated fetal bovine serum (HI-FBS; Life Technologies)). Human embryonic kidney (HEK) 293T cells (ATCC) were cultured in DMEM (HyClone) supplemented with 10% HI-FBS.

Generation of CAR-expressing primary human T cells. CD8+/CD45RA-/CD62L+ T cells were isolated from healthy donor whole blood obtained from the UCLA Blood and Platelet Center, stimulated with CD3/CD28 T-cell activation Dynabeads (Life Technologies) at a 1:1 bead:cell ratio, and lentivirally transduced 72 hours later at a multiplicity of infection of 1.5. All T cells were expanded in complete T-cell medium supplemented with 100 U/mL penicillin-streptomycin (Life Technologies) and fed 50 U/mL IL-2 (Life Technologies) and 1 ng/mL IL-15 (Miltenyi) every 48 hours. Dynabeads were removed 9 or 10 days post-isolation. CAR+ cells were enriched by magnetic bead-based sorting (Miltenyi) and expanded by stimulation with irradiated TM-LCLs at a T cell:TM-LCL ratio of 1:7. Mock-transduced T cells were stimulated using the rapid expansion protocol as previously described (20). Each *in vitro* experiment was repeated with T cells from different donors (T cells were never pooled). See Supplementary Materials and Methods for additional details.

Cytotoxicity assay. Target cells (K562 cells) seeded at $1x10^4$ cells/well in a 96-well plate were co-incubated with effector cells at varying effector-to-target (E:T) ratios in complete media without phenol red and with 5% HI-FBS for 4 hours. Supernatants were harvested and analyzed using the CytoTox 96 Non-Radioactive Cytotoxicity Assay kit (Promega).

Cytokine production quantification. Target cells were seeded at 5×10^4 cells/well in a 96-well plate and co-incubated with effector cells at an E:T ratio of 2:1 for 24 hours. Cytokine levels in the culture supernatant were measured with the BD Cytometric Bead Array Human Th1/Th2 Cytokine Kit II (BD Biosciences).

***In vivo* xenograft studies in *NOD/SCID/$\gamma_c^{-/-}$ (NSG)* mice.** All *in vivo* experiments were approved by the UCLA Institutional Animal Care and Use Committee. Six- to eight-week-old female NSG mice were bred in-house by the UCLA Department of Radiation and Oncology. Half a million EGFP+, firefly luciferase (ffLuc)-expressing Raji cells were administered to NSG mice via tail-vein injection. Seven days later, mice bearing engrafted tumors were treated with 10 x 10^6 mock-transduced or CAR+/EGFRt+ cells via tail-vein injection. Tumor progression was monitored by bioluminescence imaging using an IVIS Lumina III LT Imaging System (Perkin Elmer). Peripheral blood was obtained by retro-orbital bleeding 10 days and 20 days post tumor-cell injection, and samples were analyzed by flow cytometry.

Statistical Analysis. Statistical significance of *in vitro* results was analyzed using two-tailed, unpaired, homoscedastic Student's t-test. Survival curves were evaluated by the log-rank test, and significance was determined by comparing log-rank test statistics against a chi square table with the degree of freedom equal to one.

Results

CD19 and CD20 CARs require distinct extracellular spacer lengths

Conventional CAR molecules are comprised of four main domains: an scFv, an extracellular spacer, a transmembrane domain, and a cytoplasmic tail including co-stimulatory signals and the CD3 zeta chain (Fig. 1A). Previous work demonstrated that the CD19 CAR has superior activity when constructed with a short extracellular spacer (21), but no systematic study has been reported for CD20 CARs. Therefore, we constructed and characterized a series of CD20 CARs incorporating long (IgG4 hinge-CH2-CH3; 229 aa), medium (IgG4 hinge-CH3; 119 aa),

or short (IgG4 hinge; 12 aa) extracellular spacers connecting the Leu-16 scFv to the CD28 transmembrane domain (Supplementary Fig. S1A). All three CARs were efficiently expressed in primary CD8+ human T cells (Supplementary Fig. S1B). When challenged with CD20+ target cells, T cells expressing the long-spacer CAR consistently demonstrated greater target-cell lysis, cytokine production, and T-cell proliferation (Supplementary Fig. S1C to E), indicating functional superiority of the long-spacer CAR for CD20 detection.

Bi-specific and single-input CARs share antigen-specific structural requirements

Second-generation, CD19-OR-CD20 CARs were constructed by taking the standard four-domain CAR architecture and incorporating two scFvs connected in tandem via a G4S flexible linker (Fig. 1B). In light of the different preferences in extracellular spacer length for CD19 and CD20 single-input CARs, a panel of CD19-OR-CD20 CARs was constructed to systematically evaluate the effects of spacer length and the ordering of the two scFv domains (Fig. 1C). Each CAR was constructed in the scFv #1 (V_L-V_H) – scFv #2 (V_H-V_L) orientation to minimize potential mispairing of V_L and V_H domains between the two scFvs. All four OR-gate CARs were produced at full length and expressed on the surface of primary human CD8+ T cells (Supplementary Fig. S2A and B).

When challenged with CD19+ target cells, the OR-gate CARs showed superior cytokine production and target-cell lysis when a short extracellular spacer was used, regardless of scFv domain order (Fig. 2). Notably, both long-spacer CARs failed to produce interleukin (IL)-2 (Fig. 2A) and had minimal lysis activity against CD19+ targets (Fig. 2B). These results indicate that short-spacer CARs are more effective in targeting CD19, consistent with previously reported behavior of single-input CD19 CARs (21).

Although the long-spacer CARs failed to target CD19, they were capable of responding to CD20 (Fig. 2A). Interestingly, the 20-19 short CAR, which contained a short spacer and the CD20 scFv in the membrane-distal position, also performed well in cytokine production and demonstrated the most efficient lysis against CD20+ targets (Fig. 2). Given the scFv orientation in this construct, the CD19 scFv and the G4S linker between the two scFv domains could serve as a proxy spacer that projects the CD20 scFv away from the T-cell membrane, to a position conducive for CD20 binding. We thus hypothesized that modifying the G4S linker while keeping the 20-19 short CAR configuration may further enhance CD20 response without compromising the receptor's sensitivity toward CD19+ target cells.

Sequence modifications on scFv linkers enable effective targeting of disparate antigens

A new panel of 20-19 short CARs was constructed with various linker sequences inserted between the two scFv domains (Fig. 3A). The original, short (G4S)1 flexible linker was compared against a long (G4S)4 flexible linker, a short (EAAAK)1 rigid linker, and a long (EAAAK)3 rigid linker (22,23). CARs with modified linker sequences were expressed at full length and localized to the cell surface (Supplementary Fig. S2C and D).

To evaluate the utility of OR-gate CARs in preventing antigen escape, a mutant CD19– lymphoma cell line was generated by CRISPR/Cas9-mediated genome editing of Raji lymphoma cells (Supplementary Fig. S3). As expected, the single-input CD19 CAR-T cells showed no response to CD19– target cells (Fig. 3 B to D). In contrast, T cells expressing OR-gate CARs efficiently lysed both wildtype (WT; CD19+/CD20+) and CD19– target cells (Fig. 3D). The original OR-gate CAR with a (G4S)1 linker had lower toxicity against mutant (CD19–/CD20+) Raji compared to WT Raji, indicating sub-optimal CD20 targeting. Increasing the length and/or

rigidity of the linker sequence improved the OR-gate CARs' ability to recognize CD20, resulting in equally efficient elimination of both WT and CD19– Raji target cells (Fig. 3D).

In addition to enhanced cytotoxicity, modified OR-gate CARs expressed higher levels of activation and degranulation markers, and they produced significantly more interferon (IFN)-γ, tumor necrosis factor (TNF)-α, and IL-2 compared to the original CAR with a (G4S)1 linker (Fig. 3B and C). Notably, the OR-gate CAR with a (G4S)4 linker showed similar levels of effector output compared to the single-input CD20 CAR (Fig. 3B to D). These results indicate that linker modifications successfully compensated for impairments in CD20 targeting imposed by the short extracellular spacer, which was necessary for efficient CD19 targeting.

The increase in CD20 targeting efficiency obtained by linker modifications did not compromise CD19 targeting capability. All 20-19 short CARs, regardless of linker type, showed robust CD69, CD137, and CD107a expression when challenged with WT Raji or CD19+/CD20– K562 target cells (Supplementary Fig. S4A). Compared to the single-input CD19 CAR, OR-gate CARs triggered comparable levels of activation and degranulation marker expression as well as IFN-γ production in response to CD19 stimulation (Supplementary Fig. S4A and B). Furthermore, OR-gate CAR-T cells were capable of lysing CD19+ target cells as efficiently as single-input CD19 CAR-T cells (Supplementary Fig. S4C). Taken together, these results demonstrate that OR-gate CARs can efficiently detect and lyse CD19– escape mutants *in vitro*, and that rational modifications to the CAR structure successfully improved CD20 targeting while maintaining high CD19 sensitivity.

Bi-specificity does not affect CAR-T cell growth, differentiation, exhaustion profile, or lytic capability *in vitro*

Despite comparable activation marker expression and lytic capabilities, CD19 and OR-gate CAR-T cells showed disparate IL-2 production levels upon antigen stimulation (Supplementary Fig. S4B). To investigate potential effects of this difference in cytokine production, we examined the cell differentiation pattern and proliferation rate of the various CAR-T cell lines during extended co-incubation with Raji target cells in the absence of exogenous cytokines.

Across multiple donors, we consistently observed a slightly but statistically significantly larger central memory (T_{CM}) population among cultured CD19 CAR-T cells compared to OR-gate CAR-T cells prior to antigen stimulation (Fig. 4A). However, this statistical difference disappeared after 6 days of co-incubation with WT Raji targets, with no major fluctuation in cell-type distribution (Fig. 4A), indicating that the level of antigen-stimulated IL-2 production does not have a major impact on cell-type differentiation *in vitro*. Furthermore, CD19 and OR-gate CAR-T cells exhibit similar proliferation rates upon antigen stimulation (Fig. 4B). This result indicates that the IL-2 level produced by OR-gate CAR-T cells is sufficient to support robust T-cell proliferation, an observation that was later confirmed *in vivo* (see next section).

Interestingly, despite producing similar IL-2 levels as OR-gate CAR-T cells, CD20 CAR-T cells showed significantly weaker proliferation compared to CD19 CAR-T cells (Fig. 4B). Furthermore, when single-input CD19 and CD20 CAR-T cell lines were mixed and co-cultured with WT Raji target cells, the CD19 CAR-T cells proliferated significantly more than CD20 CAR-T cells, ultimately leading to a net decrease in the CD20 CAR–T-cell population (Fig. 4C). These results demonstrate that simultaneous administration of a mixture of two CAR–T-cell lines can result in the selective expansion of one at the expense of the other. This behavior highlights an important benefit of utilizing a single, bi-specific CAR-T cell product, which can ensure the

maintenance of both CD19 and CD20 recognition capabilities while avoiding growth competition between multiple T-cell products.

We next investigated whether the tumor-lysis capability and exhaustion profile of the OR-gate CARs differ from those of the single-input CARs in response to initial antigen stimulation and subsequent emergence of antigen-escape mutants. At a 2:1 effector-to-target (E:T) ratio, all CAR–T-cell lines eliminated WT Raji cells after 6 days (Fig. 5A), at which point each sample was re-challenged with CD19– mutant Raji cells at a 2:1 E:T ratio. Target-cell count indicated that both OR-gate and CD20 CAR-T cells efficiently eliminated CD19– targets, while CD19 CAR-T cells failed to curb the outgrowth of escape mutants (Fig. 5B). Surface antibody staining revealed consistent upregulation of PD-1, Tim-3, and Lag-3 upon antigen stimulation across all CAR constructs (Fig. 5C and Supplementary Fig. S5). Upon subsequent challenge with CD19– target cells, exhaustion marker expression was sustained in OR-gate and CD20 CAR-T cells but declined in CD19 CAR-T cells (Fig. 5C and Supplementary Fig. S5). Taken together, these results indicate that OR-gate CAR-T cells retain robust effector function upon repeated antigen presentation, and they exhibit equivalent lysis capabilities and exhaustion marker expression patterns as CD20 CAR-T cells in response to CD19– escape mutants.

OR-gate CARs prevent tumor antigen escape *in vivo*

To determine the *in vivo* functionality of OR-gate CARs, *NOD/SCID/*$\gamma_c^{-/-}$ (NSG) mice were injected with either a pure population of WT Raji cells or a 3:1 mixture of WT and CD19– Raji cells. Mice bearing established xenografts were then treated with CD8+ CAR-T cells. As expected, single-input CD19 CAR-T cells significantly extended the survival of animals engrafted with WT Raji cells but failed to control the mixed Raji population (Fig. 6 and

Supplementary Fig. S6A). Post-mortem analysis revealed the outgrowth of CD19– mutants in the mixed-Raji xenograft, confirming antigen escape from single-input CAR–T-cell therapy (Supplementary Fig. S6B).

In contrast to the single-input CD19 CAR, OR-gate CARs were able to target WT and mixed Raji tumors with equal efficiency (Fig. 6 and Supplementary Fig. S6C), demonstrating that OR-gate CAR-T cells were unaffected by the loss of CD19 expression on tumor cells and only require a single antigen to trigger robust anti-tumor functions. Furthermore, both OR-gate CARs performed as well as the single-input CD19 CAR in controlling the growth of WT Raji cells (Supplementary Fig. S6D), confirming that the broadening of antigen specificity did not compromise *in vivo* anti-tumor efficacy against CD19+ targets. Taken together, these results demonstrate that OR-gate CARs can efficiently target malignant B cells and abrogate the effects of tumor-antigen loss *in vivo*.

Although OR-gate CARs are unaffected by the loss of CD19 antigen, none of the CAR-T cell lines—including second-generation CD19 CAR-T cells challenged with WT Raji cells—were able to completely eradicate engrafted tumors under the conditions tested. Analysis of retro-orbital blood samples obtained three days post T-cell injection confirmed the presence of CAR-T cells (Fig. 7A). Furthermore, both OR-gate CAR-T cell lines showed expansion *in vivo* (Supplementary Fig. S6E). Finally, CAR-expressing T cells could be found in the bone marrow of all animals at the time of sacrifice (Fig. 7B), and all Raji cells retained either CD19 expression or CD19/CD20 dual-expression (Supplementary Fig. S7). Therefore, inability to clear the tumor burden was not due to absence of CAR–T-cell proliferation or the loss of both targeted antigens.

We next investigated the cell-type differentiation and exhaustion marker expression patterns of the CAR-T cells. Results indicate a significant increase in PD-1 expression but little

change in cell-type distribution after *in vivo* antigen exposure (Fig. 7C and D). Interestingly, PD-1 expression was significantly higher for CD19 CAR-T cells compared to OR-gate CAR-T cells (Fig. 7C). However, PD-1 is known to be upregulated upon T-cell activation, and previous work has demonstrated that prolonged PD-1 does not necessarily indicate lack of effector function in CAR-T cells (24). Given the proven clinical efficacy of the second-generation CD19 CAR, the inability to achieve tumor clearance here is likely a result of the aggressive tumor line and specific tumor and T-cell dosages evaluated in this animal study.

Discussion

CD19 CAR–T-cell therapy has yielded remarkable clinical outcomes in the treatment of acute and chronic B-cell malignancies (3-9). However, this treatment strategy's vulnerability to antigen escape has been highlighted by multiple cases of relapse resulting from the emergence of CD19– tumor cells (7,10). To arm CD19 CAR-T cells against antigen escape, we constructed novel CARs capable of OR-gate signal processing—i.e., receptors that can trigger robust T-cell responses as long as the target cells express either CD19 or CD20. Results of our *in vitro* and *in vivo* characterization experiments indicate that the CD19-OR-CD20 CARs can safeguard against the effects of antigen escape by targeting malignant B-cells through CD20 when CD19 expression has been lost.

The choice of CD19 and CD20 as the target-antigen pair provides several important advantages. First, CD19 and CD20 are both clinically validated B-cell antigens expressed on the vast majority of malignant B cells (10,25,26), making the CD19-OR-CD20 CAR a clinically applicable construct that addresses a real challenge facing adoptive T-cell therapy. Second, efforts to broaden the recognition capability of CAR-T cells are often met with the undesirable

side effect of increased on-target, off-tumor toxicity. However, this trade-off does not apply to the case of CD19 and CD20, since both are exclusively expressed on B cells and have the same off-tumor toxicity profile. Finally, the ubiquitous expression of CD19 and CD20 on B cells and their known and predicted roles in promoting B-cell survival (27,28) suggest that simultaneous loss of both antigens would be a very low-probability event. Therefore, targeting CD19 and CD20 is expected to provide an effective safeguard against antigen escape by malignant B cells.

In principle, multiple receptor configurations can be adopted to achieve bi-specific signal computation, such as co-expressing two different CARs in one T cell (29) or mixing two CAR–T-cell lines, each targeting a different antigen (30). Instead, we chose to engineer dual-antigen recognition capability into a single CAR molecule due to a number of unique advantages. First, compared to expressing two separate single-input CARs in one T cell, the bi-specific CAR has a significantly smaller DNA footprint (reduced by ~40% in DNA length), and previous studies have shown that construct size significantly impacts viral vector packaging and transduction efficiency (31,32). Most clinical T-cell products are administered as a polyclonal population without prior sorting for CAR+ cells (3,5,6), thus the ability to achieve high transduction efficiency has a direct impact on clinical efficacy. Genetic compactness becomes particularly critical when features such as suicide genes (33) and additional signal-processing units (e.g., inhibitory receptors (34)) also need to be integrated into the CAR-T cells to ensure safety or enhance efficacy. Second, compared to mixing two different single-input CAR–T-cell lines, the ability to produce and administer a single, bi-specific CAR–T-cell product significantly reduces treatment costs and increases the probability of successful T-cell production within a short clinical timeframe. Third, the CD19 CAR has outperformed all other CARs evaluated in the clinic to-date, including the CD20 CAR (35,36). Our data demonstrate that in a co-culture, CD19

CAR-T cells have a significant growth advantage over CD20 CAR-T cells, resulting in a net decline in CD20 CAR–T-cell count despite the presence of CD20 antigen (Fig. 4C). Therefore, it is probable that co-administering two single-input CAR–T-cell populations would result in the disproportionate expansion of CD19 CAR-T cells at the expense of CD20 CAR-T cells, thereby compromising this strategy's ability to safeguard against CD19– mutants when they emerge later in the treatment period. By making each T cell capable of bi-specific antigen recognition, the OR-gate CAR design maximizes the number of T cells that can recognize an escape mutant when it appears. For these reasons, we chose to engineer a single CAR molecule capable of dual-antigen recognition by attaching two tandem scFv domains to the standard CAR chassis. Our data indicate that T cells expressing OR-gate CARs are indeed insensitive to the loss of CD19 on target cells, proliferate robustly in response to either CD19 or CD20 stimulation, do not exhibit altered cell-type differentiation patterns compared to single-input CAR-T cells, and retain robust target-cell lysis capability upon repeated antigen stimulation.

CARs are frequently thought of as modular proteins whose sensor domains (i.e., the scFv) can be easily changed to alter receptor specificity. However, results from a previous report (21) and our own investigation (Supplementary Fig. S1) revealed that efficient CD19 and CD20 targeting by single-input CARs requires distinct receptor structures. These divergent preferences may be a consequence of structural differences between the two antigens: CD19 is an immunoglobulin-like molecule that belongs to a family of single-pass transmembrane proteins that project outward from the cell membrane (37); CD20 is a multi-pass transmembrane protein that lies close to the cell surface (38). To achieve the optimal conjugation distance between a T cell and its target, the receptor needs to be adjusted to match the size of the target antigen, resulting in the need for a shorter CAR when targeting antigens with extensive extracellular

domains and vice versa. Although this hypothesis is consistent with our observations, quantitative imaging studies would be required to confirm its accuracy.

Based on our understanding of the structural requirements for productive CAR/antigen interactions, we arrived at the optimal structure for a bi-specific CAR through systematic, rational design. By adjusting the extracellular spacer length and linker sequence between the two scFv domains, we were able to independently optimize CD19 and CD20 targeting without compromising the CAR's ability to recognize either antigen. *In vitro* and *in vivo* results demonstrate that the OR-gate CARs are as efficient in CD19 targeting as the clinically successful single-input CD19 CAR, and the OR-gate CARs succeed in controlling CD19– mutant lymphoma cells where the single-input CAR fails (Figs. 3 and 6). A potential concern with the design of bi-specific CARs is the increased number of peptide fusion points in the receptor protein. However, almost all of the components utilized in the OR-gate CARs presented in this study have been tested in the clinic, including the two scFv domains, the long and short extracellular spacers, as well as the transmembrane and cytoplasmic signaling domains (3-5,7,8,39). Furthermore, long, flexible linker peptides consisting of glycine and serine residues have been utilized in fusion peptides such as rVIIa-FP, which is currently in clinical trial (40,41). It remains possible that rigid peptide linkers or new combinations of previously tested peptide components could result in immunogenicity. However, available evidence suggests that the probability is low and will have to be verified through extensive testing in pre-clinical and clinical studies.

Several recent studies have explored the contribution of individual CAR components to T-cell functionality, with results suggesting that the scFv framework regions, extracellular spacer length, and co-stimulatory signals all play important and non-obvious roles in enabling robust T-

cell–mediated response to tumor antigens (21,36,42-45). It remains possible that additional modifications to each of these domains could further increase the OR-gate CAR's functionality. Increasingly detailed mechanistic understanding of CAR signaling and the systematic incorporation of such knowledge into the rational design of next-generation CAR molecules will continue to facilitate the development of more effective and predictable cell-based therapeutics.

Adoptive T-cell therapy has been hailed as one of the most promising advancements in cancer therapy in recent years, and CD19 CAR–T-cell therapy holds the spotlight as the most successful adoptive T-cell therapy to-date. The work reported here presents an effective and clinically applicable solution to the challenge of antigen escape, which has been observed in multiple clinical trials of CD19 CAR–T-cell therapy. The CD19-OR-CD20 CAR is fully compatible with current T-cell manufacturing processes, does not impose extra burden in the form of large viral packaging and transduction payloads, and enables a single T-cell product to target two clinically validated antigens associated with B-cell leukemia and lymphoma. Finally, the design principles highlighted in this study can be further utilized to construct novel CARs for additional antigen pairs to broaden the applicability and increase the efficacy of T-cell therapy for cancer.

Acknowledgments. The authors thank Lisa Rolczynski for her technical assistance. This research was funded by the National Institutes of Health (5DP5OD012133, grant to YYC; 2R01CA136551-06A1, grant to MCJ).

Author contributions: YYC and MCJ conceptualized the project. YYC and EZ designed experiments, analyzed data, and wrote the manuscript. EZ performed *in vitro* and *in vivo*

experiments; MYL performed *in vivo* experiments; AS performed *in vitro* experiments comparing CD20 single-input CARs.

References

1. Kalos M, June CH. Adoptive T cell transfer for cancer immunotherapy in the era of synthetic biology. Immunity 2013;39(1):49-60.
2. Rosenberg SA, Restifo NP. Adoptive cell transfer as personalized immunotherapy for human cancer. Science 2015;348(6230):62-8.
3. Kalos M, Levine BL, Porter DL, Katz S, Grupp SA, Bagg A, et al. T cells with chimeric antigen receptors have potent antitumor effects and can establish memory in patients with advanced leukemia. Sci Transl Med 2011;3(95):95ra73.
4. Porter DL, Levine BL, Kalos M, Bagg A, June CH. Chimeric antigen receptor-modified T cells in chronic lymphoid leukemia. N Engl J Med 2011;365(8):725-33.
5. Brentjens RJ, Davila ML, Riviere I, Park J, Wang X, Cowell LG, et al. CD19-targeted T cells rapidly induce molecular remissions in adults with chemotherapy-refractory acute lymphoblastic leukemia. Sci Transl Med 2013;5(177):177ra38.
6. Kochenderfer JN, Dudley ME, Feldman SA, Wilson WH, Spaner DE, Maric I, et al. B-cell depletion and remissions of malignancy along with cytokine-associated toxicity in a clinical trial of anti-CD19 chimeric-antigen-receptor-transduced T cells. Blood 2012;119(12):2709-20.
7. Grupp SA, Kalos M, Barrett D, Aplenc R, Porter DL, Rheingold SR, et al. Chimeric antigen receptor-modified T cells for acute lymphoid leukemia. N Engl J Med 2013;368(16):1509-18.
8. Davila ML, Riviere I, Wang X, Bartido S, Park J, Curran K, et al. Efficacy and toxicity management of 19-28z CAR T cell therapy in B cell acute lymphoblastic leukemia. Sci Transl Med 2014;6(224):224ra25.

9. Kochenderfer JN, Dudley ME, Kassim SH, Somerville RP, Carpenter RO, Stetler-Stevenson M, et al. Chemotherapy-refractory diffuse large B-cell lymphoma and indolent B-cell malignancies can be effectively treated with autologous T cells expressing an anti-CD19 chimeric antigen receptor. J Clin Oncol 2015;33(6):540-9.

10. Maude SL, Frey N, Shaw PA, Aplenc R, Barrett DM, Bunin NJ, et al. Chimeric antigen receptor T cells for sustained remissions in leukemia. N Engl J Med 2014;371(16):1507-17.

11. Rapoport AP, Stadtmauer EA, Binder-Scholl GK, Goloubeva O, Vogl DT, Lacey SF, et al. NY-ESO-1-specific TCR-engineered T cells mediate sustained antigen-specific antitumor effects in myeloma. Nat Med 2015;21(8):914-21.

12. Jager E, Ringhoffer M, Karbach J, Arand M, Oesch F, Knuth A. Inverse relationship of melanocyte differentiation antigen expression in melanoma tissues and CD8+ cytotoxic-T-cell responses: evidence for immunoselection of antigen-loss variants in vivo. Int J Cancer 1996;66(4):470-6.

13. Riker A, Cormier J, Panelli M, Kammula U, Wang E, Abati A, et al. Immune selection after antigen-specific immunotherapy of melanoma. Surgery 1999;126(2):112-20.

14. Grada Z, Hegde M, Byrd T, Shaffer DR, Ghazi A, Brawley VS, et al. TanCAR: A Novel Bispecific Chimeric Antigen Receptor for Cancer Immunotherapy. Mol Ther Nucleic Acids 2013;2:e105.

15. Gibson DG, Young L, Chuang RY, Venter JC, Hutchison CA, 3rd, Smith HO. Enzymatic assembly of DNA molecules up to several hundred kilobases. Nat Methods 2009;6(5):343-5.

16. Nicholson IC, Lenton KA, Little DJ, Decorso T, Lee FT, Scott AM, et al. Construction and characterisation of a functional CD19 specific single chain Fv fragment for immunotherapy of B lineage leukaemia and lymphoma. Mol Immunol 1997;34(16-17):1157-65.

17. Jensen M, Tan G, Forman S, Wu AM, Raubitschek A. CD20 is a molecular target for scFvFc:zeta receptor redirected T cells: implications for cellular immunotherapy of CD20+ malignancy. Biol Blood Marrow Transplant 1998;4(2):75-83.

18. Wang X, Chang WC, Wong CW, Colcher D, Sherman M, Ostberg JR, et al. A transgene-encoded cell surface polypeptide for selection, in vivo tracking, and ablation of engineered cells. Blood 2011;118(5):1255-63.

19. Pelloquin F, Lamelin JP, Lenoir GM. Human B lymphocytes immortalization by Epstein-Barr virus in the presence of cyclosporin A. In Vitro Cell Dev Biol 1986;22(12):689-94.

20. Riddell SR, Greenberg PD. The use of anti-CD3 and anti-CD28 monoclonal antibodies to clone and expand human antigen-specific T cells. J Immunol Methods 1990;128(2):189-201.

21. Hudecek M, Sommermeyer D, Kosasih PL, Silva-Benedict A, Liu L, Rader C, et al. The nonsignaling extracellular spacer domain of chimeric antigen receptors is decisive for in vivo antitumor activity. Cancer Immunol Res 2015;3(2):125-35.

22. Arai R, Ueda H, Kitayama A, Kamiya N, Nagamune T. Design of the linkers which effectively separate domains of a bifunctional fusion protein. Protein Eng 2001;14(8):529-32.

23. Arai R, Wriggers W, Nishikawa Y, Nagamune T, Fujisawa T. Conformations of variably linked chimeric proteins evaluated by synchrotron X-ray small-angle scattering. Proteins 2004;57(4):829-38.

24. Chang ZL, Silver PA, Chen YY. Identification and selective expansion of functionally superior T cells expressing chimeric antigen receptors. J Transl Med 2015;13:161.

25. Boye J, Elter T, Engert A. An overview of the current clinical use of the anti-CD20 monoclonal antibody rituximab. Ann Oncol 2003;14(4):520-35.

26. Till BG, Jensen MC, Wang J, Qian X, Gopal AK, Maloney DG, et al. CD20-specific adoptive immunotherapy for lymphoma using a chimeric antigen receptor with both CD28 and 4-1BB domains: pilot clinical trial results. Blood 2012;119(17):3940-50.

27. Otero DC, Anzelon AN, Rickert RC. CD19 function in early and late B cell development: I. Maintenance of follicular and marginal zone B cells requires CD19-dependent survival signals. J Immunol 2003;170(1):73-83.

28. Tedder TF, Engel P. CD20: a regulator of cell-cycle progression of B lymphocytes. Immunol Today 1994;15(9):450-4.

29. Hegde M, Corder A, Chow KK, Mukherjee M, Ashoori A, Kew Y, et al. Combinational targeting offsets antigen escape and enhances effector functions of adoptively transferred T cells in glioblastoma. Mol Ther 2013;21(11):2087-101.

30. Anurathapan U, Chan RC, Hindi HF, Mucharla R, Bajgain P, Hayes BC, et al. Kinetics of tumor destruction by chimeric antigen receptor-modified T cells. Mol Ther 2014;22(3):623-33.

31. Bos TJ, De Bruyne E, Van Lint S, Heirman C, Vanderkerken K. Large double copy vectors are functional but show a size-dependent decline in transduction efficiency. J Biotechnol 2010;150(1):37-40.

32. Kumar M, Keller B, Makalou N, Sutton RE. Systematic determination of the packaging limit of lentiviral vectors. Hum Gene Ther 2001;12(15):1893-905.

33. Zhou X, Dotti G, Krance RA, Martinez CA, Naik S, Kamble RT, et al. Inducible caspase-9 suicide gene controls adverse effects from alloreplete T cells after haploidentical stem cell transplantation. Blood 2015;125(26):4103-13.

34. Fedorov VD, Themeli M, Sadelain M. PD-1- and CTLA-4-based inhibitory chimeric antigen receptors (iCARs) divert off-target immunotherapy responses. Sci Transl Med 2013;5(215):215ra172.

35. Gill S, June CH. Going viral: chimeric antigen receptor T-cell therapy for hematological malignancies. Immunol Rev 2015;263(1):68-89.

36. Long AH, Haso WM, Shern JF, Wanhainen KM, Murgai M, Ingaramo M, et al. 4-1BB costimulation ameliorates T cell exhaustion induced by tonic signaling of chimeric antigen receptors. Nat Med 2015;21(6):581-90.

37. Tedder TF, Isaacs CM. Isolation of cDNAs encoding the CD19 antigen of human and mouse B lymphocytes. A new member of the immunoglobulin superfamily. J Immunol 1989;143(2):712-7.

38. Einfeld DA, Brown JP, Valentine MA, Clark EA, Ledbetter JA. Molecular cloning of the human B cell CD20 receptor predicts a hydrophobic protein with multiple transmembrane domains. EMBO J 1988;7(3):711-7.

39. Till BG, Jensen MC, Wang J, Chen EY, Wood BL, Greisman HA, et al. Adoptive immunotherapy for indolent non-Hodgkin lymphoma and mantle cell lymphoma using genetically modified autologous CD20-specific T cells. Blood 2008;112(6):2261-71.

40. Weimer T, Wormsbacher W, Kronthaler U, Lang W, Liebing U, Schulte S. Prolonged in-vivo half-life of factor VIIa by fusion to albumin. Thromb Haemost 2008;99(4):659-67.

41. Zollner S, Schuermann D, Raquet E, Mueller-Cohrs J, Weimer T, Pragst I, et al. Pharmacological characteristics of a novel, recombinant fusion protein linking coagulation factor VIIa with albumin (rVIIa-FP). J Thromb Haemost 2014;12(2):220-8.

42. Guest RD, Hawkins RE, Kirillova N, Cheadle EJ, Arnold J, O'Neill A, et al. The role of extracellular spacer regions in the optimal design of chimeric immune receptors: evaluation of four different scFvs and antigens. J Immunother 2005;28(3):203-11.

43. Hudecek M, Lupo-Stanghellini MT, Kosasih PL, Sommermeyer D, Jensen MC, Rader C, et al. Receptor affinity and extracellular domain modifications affect tumor recognition by ROR1-specific chimeric antigen receptor T cells. Clin Cancer Res 2013;19(12):3153-64.

44. Frigault MJ, Lee J, Basil MC, Carpenito C, Motohashi S, Scholler J, et al. Identification of chimeric antigen receptors that mediate constitutive or inducible proliferation of T cells. Cancer Immunol Res 2015;3(4):356-67.

45. Kunkele A, Johnson AJ, Rolczynski LS, Chang CA, Hoglund V, Kelly-Spratt KS, et al. Functional Tuning of CARs Reveals Signaling Threshold above Which CD8+ CTL Antitumor Potency Is Attenuated due to Cell Fas-FasL-Dependent AICD. Cancer Immunol Res 2015;3(4):368-79.

Figure Legends

Fig. 1: Schematics of single-input and bi-specific CARs. A, a second-generation, single-input CAR. B, a bi-specific, OR-gate CAR. C, schematic of four OR-gate CARs containing variations in extracellular spacer length and ordering of scFv domains. Hinge, CH2, and CH3 are domains within human IgG4. CD28tm is the CD28 transmembrane domain. EGFRt was fused to all CAR constructs via a T2A cleavage peptide to facilitate staining for CAR expression and sorting.

Fig. 2: Functional CD19-OR-CD20 CARs can be constructed by linking scFv domains in tandem. A, IFN-γ, TNF-α, and IL-2 production by T cells expressing single-input or OR-gate CARs. Cytokine levels in media were measured after a 24-hour co-incubation with K562 target cells. B, target-cell lysis activity of CD19-OR-CD20 CARs following a 4-hour co-incubation with K562 target cells. Reported values are the mean of triplicates, with error bars indicating one standard deviation (SD).

Fig. 3: Rational structural modifications improve OR-gate CAR activity against mutant tumor cells. A, design of 20-19 Short CARs incorporating linkers with increased length and/or rigidity. B, CD69, CD137, and CD107a surface expression (in median fluorescence intensity; MFI) by CAR-T cells after a 24-hour co-incubation with CD19– Raji cells. C, IFN-γ, TNF-α, and IL-2 production by the CAR-T cells in (B). D, cell lysis by single-input and OR-gate CAR-T cells after 4-hour co-incubation with WT and CD19– Raji cells. Reported values are the mean of triplicates, with error bars indicating one SD. *P*-values were calculated by two-tailed Student's *t* test; *: $p < 0.05$; **: $p < 0.01$.

Fig. 4: CD19 and OR-gate CAR T-cells exhibit similar differentiation and cell proliferation following antigen stimulation. A, distribution of T-cell subtypes prior to co-incubation with WT Raji cell targets and 6 days post target-cell addition. Cells were surface- stained for CD45RA and CCR7 expression. B, T-cell proliferation after co-incubation with WT Raji cells. CD19 and OR-gate CAR-T cells show similar proliferation while CD20 CAR-T cells show significantly less proliferation compared to CD19 CAR-T cells ($p < 0.01$ for all time points except for day 6). C, expansion of mixed CD19 and CD20 CAR-T cells stimulated with WT Raji cells over 8 days. Values shown are the mean of triplicates, with error bars indicating one SD. *P*-values were calculated by two-tailed Student's *t* test; n.s.: not significant ($p > 0.1$); *: $p < 0.05$; **: $p < 0.01$.

Fig. 5: OR-gate CAR-T cells maintain robust lysis capability through repeated antigen stimulation. Mock-transduced and CAR-T cells were co-incubated with WT Raji targets for 6 days, and then co-incubated with CD19– mutant Raji targets for another 6 days. A, survival of WT Raji cells co-incubated with effector T cells. B, survival of CD19– Raji cells co-incubated with T cells that were previously challenged with WT Raji cells. (Note: mock-transduced T cells had been overwhelmed by WT Raji by day 6 and were not re-challenged with mutant Raji.) C, Exhaustion marker staining of CAR-T cells before antigen stimulation, 48 hours after co-incubation with WT Raji (Day 2), and 48 hours or 6 days after subsequent co-incubation with CD19– Raji cells (Days 8 and 12, respectively). At each time point, cells were surface-stained for Lag-3, Tim-3, and PD-1 and then analyzed for the simultaneous expression of one, two or three markers. Values shown are the mean of triplicates, with error bars indicating one SD.

Fig. 6: OR-gate CARs abrogate the effects of antigen escape *in vivo*. A, tumor progression in NSG mice bearing WT or mixed (75% WT, 25% CD19–) Raji xenografts. Bioluminescence imaging was performed on days 6, 18, and 21 post tumor injection (T cells were injected on day 7). B, survival of mice bearing mixed Raji tumor xenografts and treated with T cells expressing no CAR, the single-input CD19 CAR, or OR-gate CARs. N = 5 in all test groups. *P*-values were calculated by log-rank test analysis; n.s.: not significant ($p > 0.1$); *: $p < 0.1$; **: $p < 0.05$.

Fig. 7: CD19 and OR-gate CAR-T cells persist, upregulate PD-1, and exhibit similar differentiation subtypes *in vivo*. A, presence of CAR-T cells in peripheral blood 3 days after T-cell injection. Cells from retro-orbital blood were stained for the expression of human CD8 and EGFRt, which was co-translated with each CAR as a T2A fusion. B, percentage of CAR-T cells present in the bone marrow collected at the time of sacrifice. C, PD-1 expression of CAR-T cells in the bone marrow of animals bearing WT Raji tumors. D, pre-injection and post-mortem T-cell subtype distributions. “WT Raji” and “Mixed Raji” labels indicate the type of tumor engrafted in the animal from which the T cells were harvested. *P*-values were calculated by two-tailed Student’s *t* test; n.s.: not significant ($p > 0.1$); *: $p < 0.05$; **: $p < 0.01$.

Figure 1

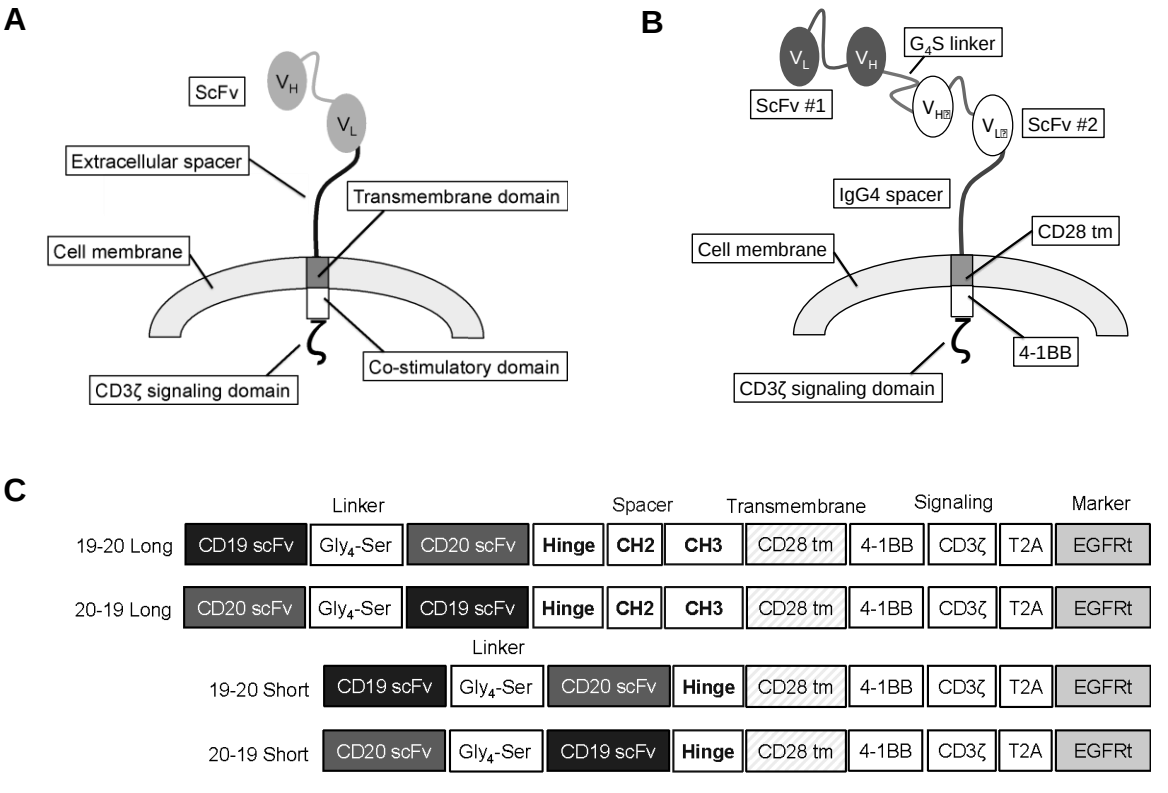
A
ScFv
V_H
V_L
Extracellular spacer
Transmembrane domain
Cell membrane
Co-stimulatory domain
CD3ζ signaling domain
B
V_L
V_H
G_4S linker
ScFv #1
V_H
V_L
ScFv #2
IgG4 spacer
CD28 tm
Cell membrane
4-1BB
CD3ζ signaling domain
C
Linker
Spacer
Transmembrane
Signaling
Marker
19-20 Long
CD19 scFv
Gly_4-Ser
CD20 scFv
Hinge
CH2
CH3
CD28 tm
4-1BB
CD3ζ
T2A
EGFRt
20-19 Long
CD20 scFv
Gly_4-Ser
CD19 scFv
Hinge
CH2
CH3
CD28 tm
4-1BB
CD3ζ
T2A
EGFRt
Linker
19-20 Short
CD19 scFv
Gly_4-Ser
CD20 scFv
Hinge
CD28 tm
4-1BB
CD3ζ
T2A
EGFRt
20-19 Short
CD20 scFv
Gly_4-Ser
CD19 scFv
Hinge
CD28 tm
4-1BB
CD3ζ
T2A
EGFRt

Figure 2

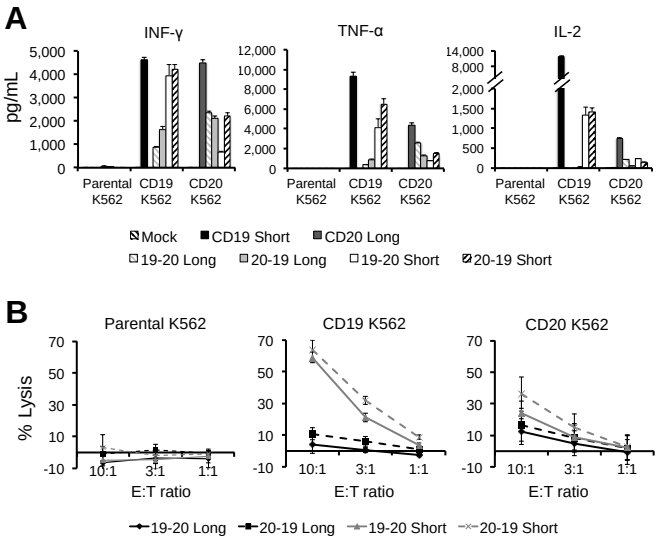
A
INF-γ
TNF-α
IL-2
pg/mL
5,000
4,000
3,000
2,000
1,000
0
12,000
10,000
8,000
6,000
4,000
2,000
0
14,000
8,000
2,000
1,500
1,000
500
0
Parental K562
CD19 K562
CD20 K562
Mock
CD19 Short
CD20 Long
19-20 Long
20-19 Long
19-20 Short
20-19 Short

B
Parental K562
CD19 K562
CD20 K562
% Lysis
70
50
30
10
-10
10:1
3:1
1:1
E:T ratio
19-20 Long
20-19 Long
19-20 Short
20-19 Short

Figure 3

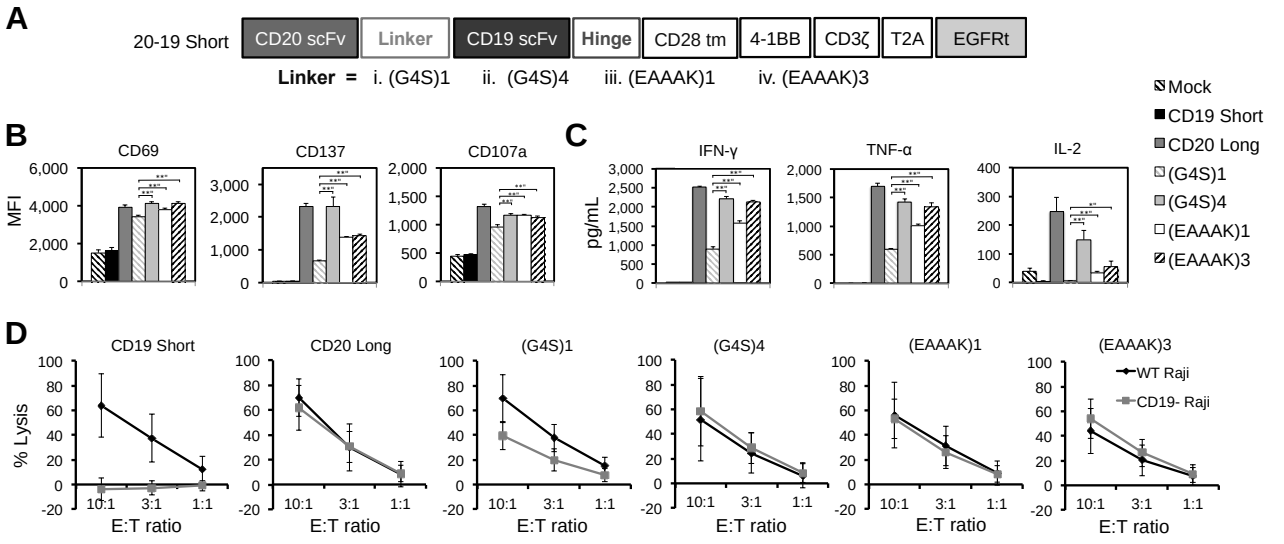
A
20-19 Short
CD20 scFv
Linker
CD19 scFv
Hinge
CD28 tm
4-1BB
CD3ζ
T2A
EGFRt
Linker = i. (G4S)1 ii. (G4S)4 iii. (EAAAK)1 iv. (EAAAK)3
B
CD69
CD137
CD107a
MFI
C
IFN-γ
TNF-α
IL-2
pg/mL
Mock
CD19 Short
CD20 Long
(G4S)1
(G4S)4
(EAAAK)1
(EAAAK)3
D
CD19 Short
CD20 Long
(G4S)1
(G4S)4
(EAAAK)1
(EAAAK)3
% Lysis
E:T ratio
10:1
3:1
1:1
WT Raji
CD19- Raji

Figure 4

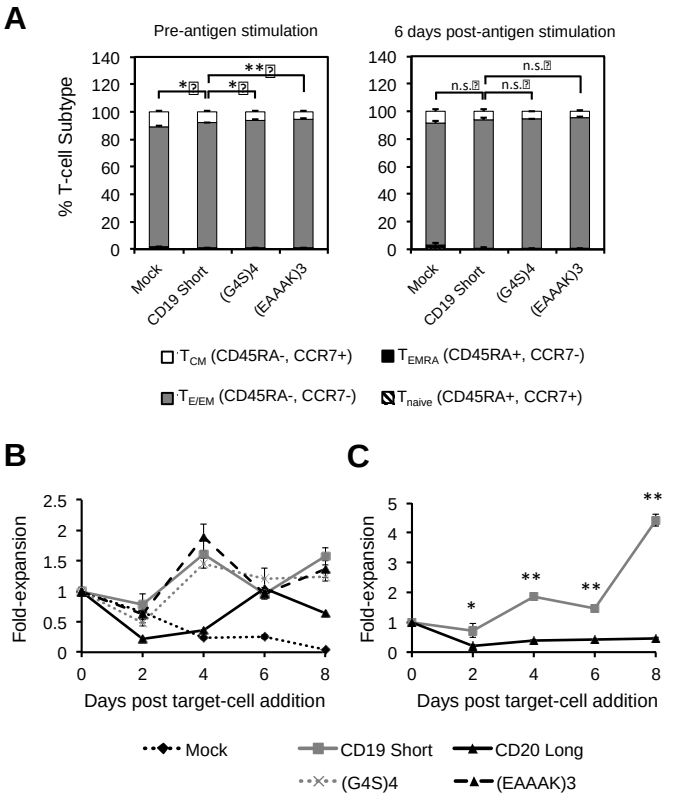
A
Pre-antigen stimulation
6 days post-antigen stimulation
% T-cell Subtype
140
120
100
80
60
40
20
0
*
*
**
n.s.
n.s.
n.s.
Mock
CD19 Short
(G4S)4
(EAAAK)3
T_CM (CD45RA-, CCR7+)
T_EMRA (CD45RA+, CCR7-)
T_E/EM (CD45RA-, CCR7-)
T_naive (CD45RA+, CCR7+)

B
C
Fold-expansion
2.5
2
1.5
1
0.5
0
0
2
4
6
8
Days post target-cell addition
5
4
3
2
1
0
*
**
**
**
Mock
CD19 Short
CD20 Long
(G4S)4
(EAAAK)3

Figure 5

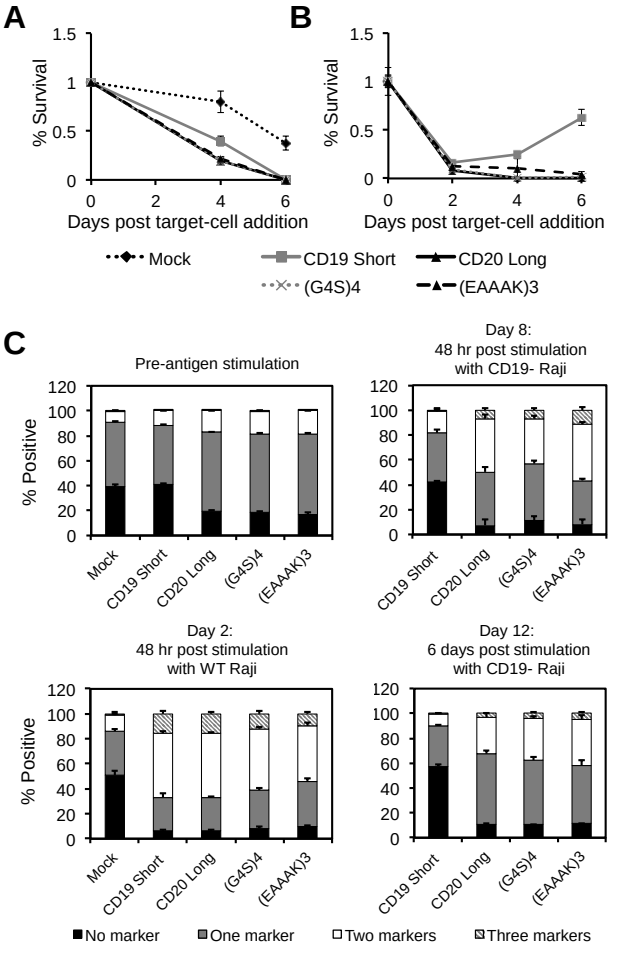
A
B
% Survival
Days post target-cell addition
Mock
CD19 Short
CD20 Long
(G4S)4
(EAAAK)3
C
Pre-antigen stimulation
Day 8:
48 hr post stimulation
with CD19- Raji
Day 2:
48 hr post stimulation
with WT Raji
Day 12:
6 days post stimulation
with CD19- Raji
% Positive
No marker
One marker
Two markers
Three markers

Figure 6

A

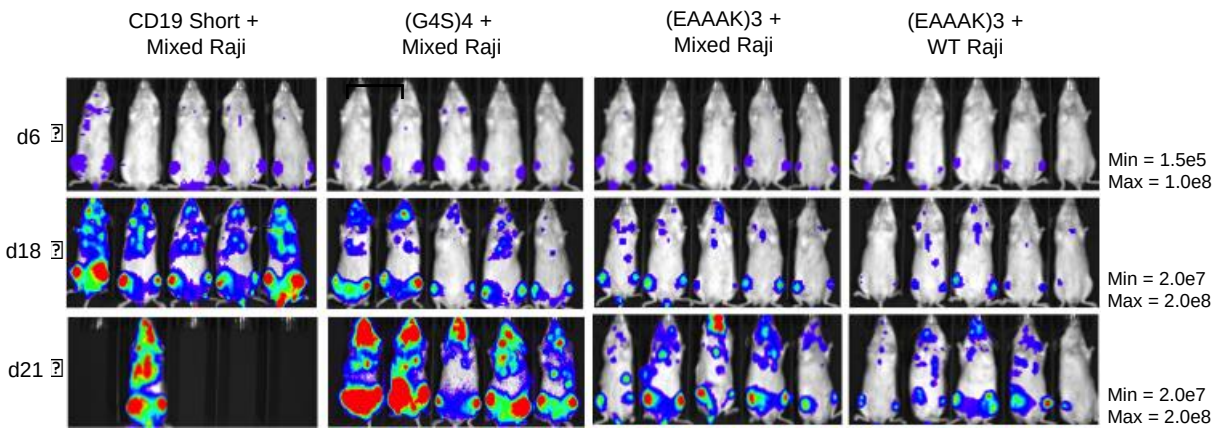
CD19 Short + Mixed Raji
(G4S)4 + Mixed Raji
(EAAAK)3 + Mixed Raji
(EAAAK)3 + WT Raji
d6
d18
d21
Min = 1.5e5
Max = 1.0e8
Min = 2.0e7
Max = 2.0e8
Min = 2.0e7
Max = 2.0e8

B

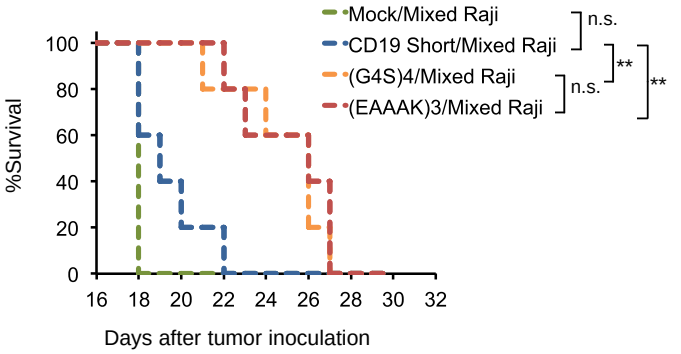
Mock/Mixed Raji
CD19 Short/Mixed Raji
(G4S)4/Mixed Raji
(EAAAK)3/Mixed Raji
n.s.
**
n.s.
**
%Survival
100
80
60
40
20
0
16
18
20
22
24
26
28
30
32
Days after tumor inoculation

Figure 7

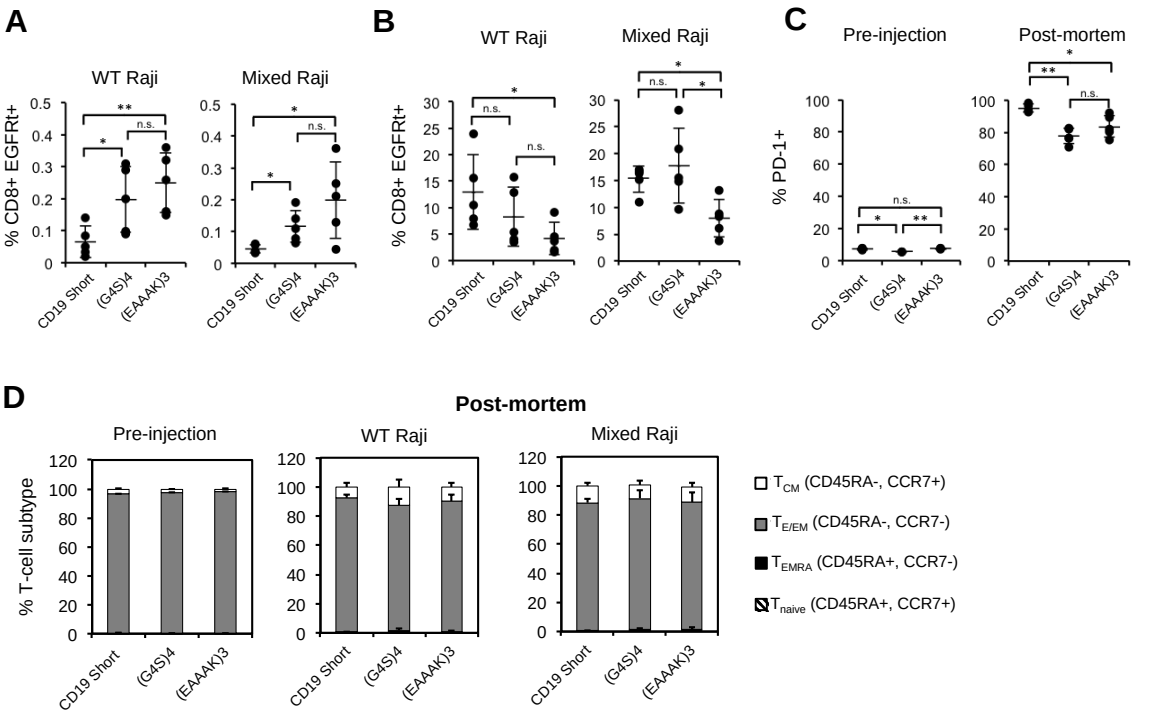
A
WT Raji
Mixed Raji
% CD8+ EGFRt+
CD19 Short
(G4S)4
(EAAAK)3
B
WT Raji
Mixed Raji
% CD8+ EGFRt+
C
Pre-injection
Post-mortem
% PD-1+
D
Post-mortem
Pre-injection
WT Raji
Mixed Raji
% T-cell subtype
T_CM (CD45RA-, CCR7+)
T_E/EM (CD45RA-, CCR7-)
T_EMRA (CD45RA+, CCR7-)
T_naive (CD45RA+, CCR7+)